Int. J. Electrochem. Sci., 15 **(2020)** 11821 – 11832, doi: 10.20964/2020.12.10

International Journal of
ELECTROCHEMICAL
SCIENCE
www.electrochemsci.org

Preparation of NiP-WC Composite Coatings by Ultrasonically Assisted Electroless Plating and Their Characterization

Xing-Shou Zhang[1], *Qin-Ying Wang*[1,*], *Yi-Rong Tang*[1], *Hai-chang Guo*[2], *Yu-chen Xi*[1], *Li-Jin Dong*[1], *Huaibei Zheng*[3]

[1] School of New energy and Materials, Southwest Petroleum University, Chengdu 610500, China
[2] Department of Materials Science and Engineering, College of Engineering, Peking University, Beijing 100871, China
[3] State Key Laboratory of Marine Equipment Made of Metal Material and Application, Anshan 114009, Chin
[*]E-mail: wangqy0401@126.com

Received: 7 April 2020 / *Accepted:* 7 June 2020 / *Published:* 31 October 2020

To improve coating properties, NiP-WC and NiP coatings have been prepared by ultrasonically assisted electroless plating and their performance after heat treatment has been studied. The surface micromorphologies of the coatings were analyzed, and it was shown that the size of the spherical microstructure of the ultrasonically assisted electroless NiP coating was reduced from 5 ~ 10μm to 2 ~ 5 μm. In addition, pure NiP and NiP-WC coatings with ultrasonic assistance showed 36% and 75% higher hardness than those without ultrasonic assistance and the hardness of the electroless coating after heat treatment was higher than that of the original electroless plating coating. The corrosion resistance of the NiP-WC and NiP electroless plating with ultrasonic assistance showed 18.46% and 52.12% higher R_p value than those without ultrasonic assistance. The results show that ultrasonic assistance can increase the uniformity, hardness, and corrosion resistance of the coating.

Keyword: NiP-WC composite coating; Ultrasonically assisted electroless plating; Heat treatment; Hardness; Corrosion behavior

1. INTRODUCTION

Carbon steels have been applied in automobiles and petroleum due to its moderate carbon content and comprehensive performance [1]. However, new requirements for the corrosion resistance of carbon steels have been proposed in more demanding environments. Many ways have been used to enhance the corrosion resistance of carbon steels, such as micro-arc oxidation [2], electroplating [3], and electroless plating [4]. Among these methods, electroless plating based on principles of automatic catalytic redox reactions to deposit amorphous coatings on activated surfaces, has been widely used in the electronics,

chemical, petroleum, and automotive industries, primarily to increase corrosion resistance and wear resistance of the surface [5-9]. Therefore, Ni-P electroless plating has been researched in the manufacturing industry. However, the Ni-P electroless plating has been unable to show higher performance in the rapid development of world manufacturing, so Ni-W-P [10], Ni-Cu-P [11], and Ni-P/SiC [12] systems have been developed. In addition, many ceramic powders have been successfully prepared for electroless plating [13-18]. Some experiments have illustrated that Ni-P composite electroless plating has higher corrosion resistance compared to Ni-P electroless plating [19].

The conventional electroless plating process is plated at 90 ^{o} C, which consumes energy, evaporates water quickly, ages the bath quickly, and lowers the utilization rate of the sodium hypophosphite reducing agent [20]. In addition, conventional electroless plating has a large porosity and high numbers of defects, which limits its application. Therefore, ultrasonically assisted electroless plating has been widely studied. Ultrasonic energy is introduced into electroless plating as a special energy input form, which can reduce the plating temperature, and energy consumption and improve the surface quality of the coating [21]. However, intensive research on the preparation and properties of ultrasonically assisted NiP-WC electroless plating is still scarce. In particular, the mechanism of ultrasonic assistance on particles in composite coatings is unclear.

This paper reports that NiP-WC and NiP coatings have been prepared by ultrasonically assisted electroless plating. The microstructure, hardness and corrosion resistance of the electroless plating coatings have been studied. This experiment was designed to investigate the performance of coatings with and without ultrasonic assistance.

2. MATERIALS AND EXPERIMENTAL METHOD

2.1 Materials

NiP-WC composite coatings were prepared on Q235 carbon steel by electroless plating with and without ultrasonic assistance. The composition of Q235 carbon steel is listed in Table 1. The composition of the plating solution was determined by considering the basic mechanism of electroless plating and long-term experience, as shown in Table 2. Among the above chemicals, $NaH_2PO_2 \cdot H_2O$ worked a as reducing agent to promote the reactions of $H_2PO^{2-} + H_2O \rightarrow HPO_3^{2-} + H^+ + 2H$ and $H_2PO^{2-} + H \rightarrow H_2O + OH^- + P$ to help form Ni-P coating; $NiSO_4 \cdot 6H_2O$ provided nickel for Ni-P coating; $C_2H_3O_2Na$ worked as a complexing agent to control the reaction rate; CH_4N_2S was used as a stabilizer to induce stability in the plating solution; $C_6H_8O_7 \cdot H_2O$ was applied to adjust the pH of the plating solution; SDS (Sodium dodecyl sulfate) was used a surfactant to prevent agglomeration of nano WC particles.

Table 1. Chemical compositions of Q235 carbon steel.

	Elements	Fe	Si	Mn	S	P	C
Q235 carbon steel	Content (wt. %)	Bal.	0.37	0.08	0.04	0.04	0.16

Table 2. Conditions of the plating solution and technological parameters of electroless plating

plating solution	content/volume	technological parameters
$NiSO_4 \cdot 6H_2O$	20 g/L	
$NaH_2PO_2 \cdot H_2O$	24 g/L	
$C_6H_8O_7 \cdot H_2O$	8 g/L	
$C_2H_3O_2Na$	10 g/L	pH: 4.0~4.5
CH_4N_2S	5m g/L	temperature 85±1°C
The mixed solution (WC, ~0.4 μm) (WC: 50 g/L, SDS: 10 g/L, deionized water: Bal.)	20 mL	stirring speed 200 r/min
The mixed solution (WC, ~0.4 μm) (WC: 50 g/L, SDS: 10 g/L, deionized water: Bal.)	20 mL	ultrasonic assistance (40 kHz)

Table 3. Preparing conditions of the achieved coatings

Coating	reaction time/min	solution volume/mL	technology	heat treatment temperature/ ^{o} C	heat treatment time/min
NiP	15	280	stirring		
NiP-WC	45	300	stirring		
NiP-UA	15	280	ultrasonic assistance		
NiP-WC-UA	45	300	ultrasonic assistance		
NiP-heat	15	280	stirring	400	60
NiP-WC-heat	45	300	stirring	400	60
NiP-UA-heat	15	280	ultrasonic assistance	400	60
NiP-WC-UA-heat	45	300	ultrasonic assistance	400	60

Prior to the experiment, the steel surface was ground and polished. Then, the specimen was ultrasonically cleaned by deionized water, ethanol, and acetone accordingly. Next, the surface of the steel was etched by hydrochloric acid (15 wt. %) by referring to the research of Luo [22]. It was rinsed by deionized water, and the sample was immersed in the electroless plating solution (280 mL) successively. First, a pure Ni-P layer was obtained on the surface of the steel after 15 min, then a mixed solution (WC: 50 g/L, SDS: 10 g/L, deionized water: Bal.) with the volume of 20 mL was gradually added to the stirred plating solution for 30 minutes to prepare a second NiP-WC layer. Consequently, a NiP-WC composite coating was achieved with a stirred plating solution. Meanwhile, the same preparation processing was repeated with the ultrasonically assisted generator (40 kHz) rather than

stirring, and a NiP-WC-UA was finally achieved. For comparison, pure NiP coatings were prepared with (NiP-UA) and without ultrasonic assistance, as shown in Table 3. In addition, all achieved coatings were heated at 400 ^{o} C for 1h to study the performance after heat treatment.

2.2 Experimental method

A scanning electron microscope (SEM, EV0 MA15 ZEISS) was applied to observe the micromorphology and measure the elemental composition of the coatings. An X-ray diffractometer (XRD, X Pert PRO MPD) was used to measure the phase compositions of the coatings over a scanning range of 20 ° to 80 °. A Vickers hardness tester (HXD-2000TM/LCD, Baoleng) was employed to research the hardness of the coating surface.

Electrochemical impedance spectroscopy (EIS) was tested in from 100 kHz to 10 MHz in 3.5 wt.% NaCl solution by an electrochemical workstation (CS310, Corrtest) at room temperature. The polarization curve of the coating was tested at stable open circuit potential (OCP) achieved after an immersion time of 2 h with a potential scanning rate of 1 mV/s. A conventional three-electrode cell was employed.

3. RESULTS AND DISCUSSION

3.1 Microstructure and compositions

The morphologies of the pure NiP and NiP-UA coatings and NiP-WC and NiP-WC-UA composite coatings were observed and presented in Fig. 1. They indicate that the surface morphology of the pure NiP-UA coating was more uniform than that of the pure NiP coating. The average size of the spherical microstructure in the NiP-UA coating was reduced to 2 ~ 5 μm from 5 ~ 10 μm in the NiP coating. In addition, the WC particles can be seen on both surfaces of the NiP-WC and NiP-WC-UA coatings. However, the particles were equally distributed on the NiP-WC-UA coating, while there was partial agglomeration on the NiP-WC coating. The above features of the morphologies in the NiP-WC-UA coating are ascribed to the cavitation, mechanical, and thermal effects induced by ultrasonication. It is helpful to disperse WC particles and metallic ions in the plating solution and promote the formation of uniform and dense coatings.

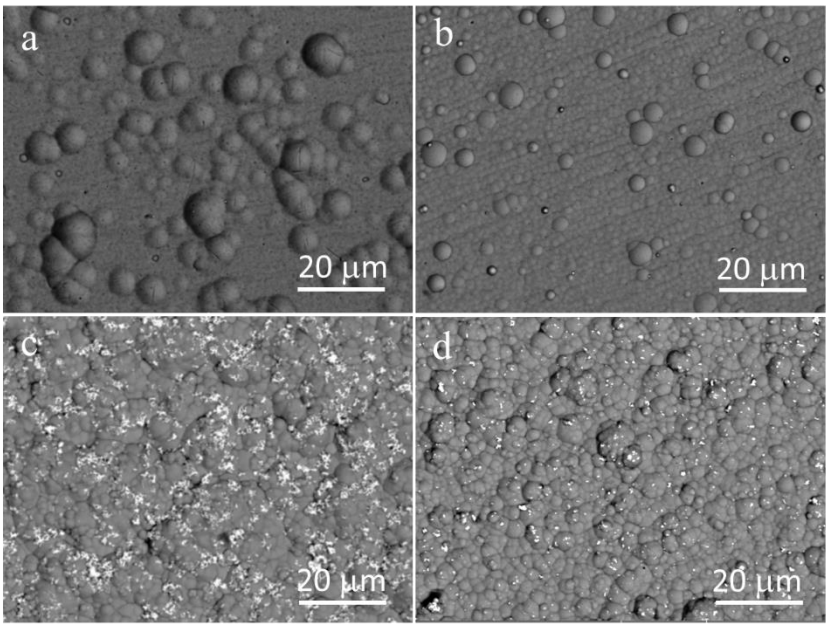

Figure 1. Surface microstructures of NiP coatings (a, b) and NiP-WC coatings (c, d) prepared by electroless plating (a, c) and ultrasonically assisted electroless plating (b, d)

The XRD patterns of all the achieved coatings, NiP, and NiP-WC, are provided in Fig. 2. The XRD pattern of the NiP coating was found to have broad diffraction peaks from 40 ° ~ 50 °. This indicates that the NiP electroless plating coating was amorphous. In addition, it is noted that the characteristic peaks of WC are found in NiP-WC coatings, revealing the successful preparation of composite coatings.

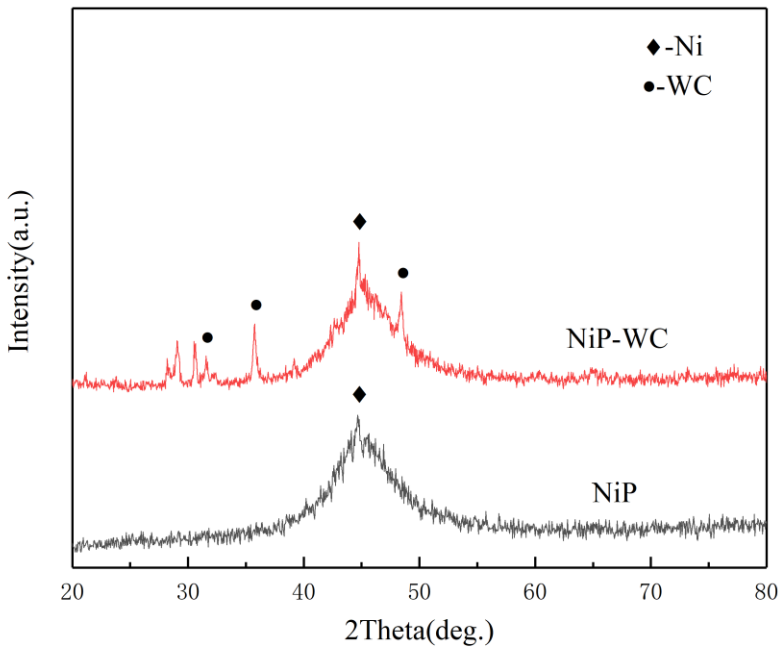

Figure 2. XRD patterns of NiP coatings and NiP-WC coatings

The thicknesses of the NiP-WC composite coatings with and without ultrasonic assistance are provided in Fig. 3. The results show that the thickness of the NiP layer for both coatings is around 4 μm (prepared for 15 min), implying that the growth of the pure NiP layer was rarely affected by ultrasonic assistance. However, the thickness of the NiP-WC layer for the ultrasonically assisted electroless plating NiP-WC composite coating is around 5 μm (prepared for 30 min), which is 3 μm large (prepared for 30 min) than the electroless plating NiP-WC composite coating. This indicates that the addition of WC particles slows the growth of NiP-WC composite coatings regardless of ultrasonic assistance. Meanwhile, ultrasonic assistance can reduce the effects of WC particles on the growth by promoting dispersion.

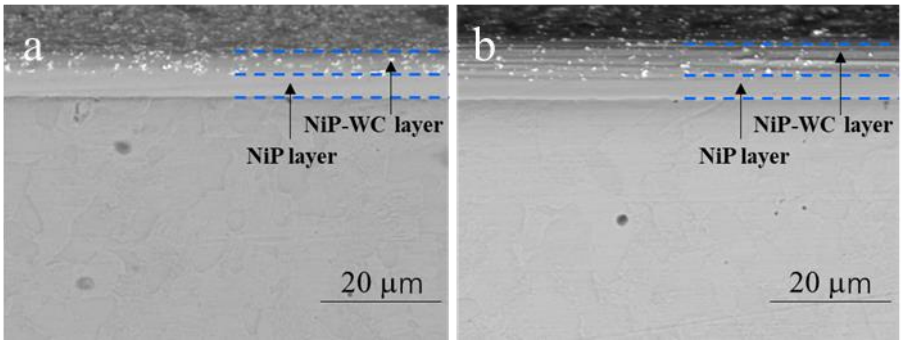

Figure 3. Thickness of NiP coatings and NiP-WC coatings prepared by electroless plating (a) and ultrasonically assisted electroless plating (b)

3.2 Hardness

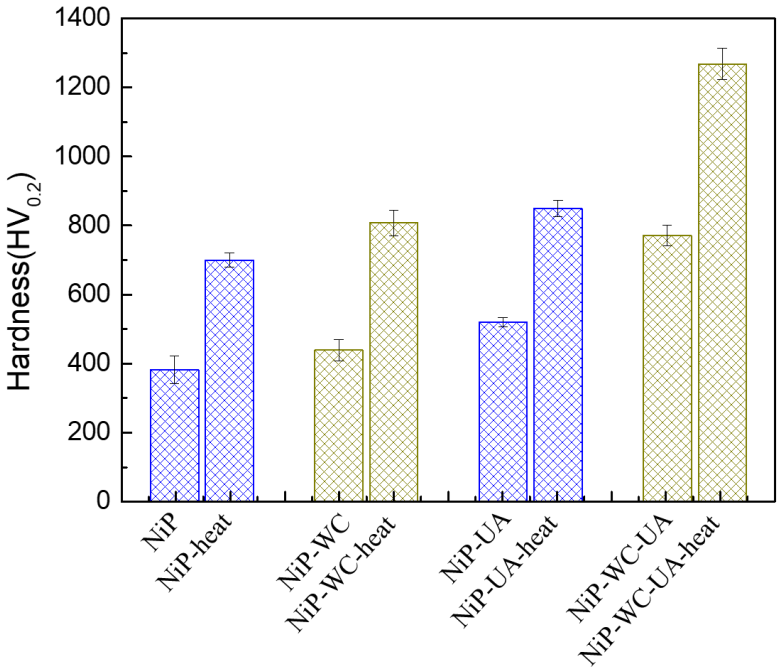

Figure 4. Vickers hardness of NiP coatings and NiP-WC coatings

The hardnesses of the coating were tested and shown in Fig. 4. Generally, the coatings after heat treatment displayed 63% ~ 84% higher hardness than that of the original coatings. This result is primarily due to the formation of the crystalline structure from the amorphous structure during heat treatment, which is helpful to improve the coating hardness [23]. Meanwhile, the addition of WC particles to the NiP matrix is helpful to improve the hardness by 15%. Pure NiP and NiP-WC coatings with ultrasonic assistance show 36% and 75% higher hardness than those without ultrasonic assistance, respectively. This is ascribed to the denser microstructures of the coatings prepared by ultrasonically assisted electroless plating.

3.3 Corrosion behavior

The Nyquist plots of the electroless plating coatings have been presented in Fig. 5. Generally, the radii of the capacitive loop coatings after heat treatment are larger than those of the untreated coatings. This reveals that the corrosion resistance of the coating has been improved after heat treatment. It means that the corrosion resistance of the crystalline coatings is higher than that of the amorphous coatings, which is not consistent with other research [24]. Commonly, the amorphous structure is more resistant to corrosion than a crystalline structure [25]. The higher corrosion resistance of the crystalline coatings found in this study is mainly ascribed to the denser microstructure after heat treatment, where the effect on the corrosion behavior of coatings is more significant than that of crystal transition. In addition, the radii of the capacitive loops of the coatings prepared with ultrasonic assistance are generally larger than the corresponding coatings without ultrasonic assistance. This is likely due to the more uniform and denser microstructure of the pure NiP coatings and more uniform distribution of WC particles in the NiP based composite coatings.

An equivalent circuit shown in Fig. 5 was employed to fit the typical Nyquist plots in Fig. 5. In this equivalent circuit, R_s is the resistance of the electrolyte. R_c and CPE_c are pore resistance and a constant phase element, respectively, to represent the surface coating. The CPE_c of this test is not an ideal capacitor because it is affected by factors such as distributed surface reactivity, roughness, electrode porosity, etc [26]. R_{ct} and C_{dl} represent the resistance of the steel substrate/electrolyte interface. The steel substrate /electrolyte interface is exposed to the electrolyte. The impedances are described by formulas (1) – (4), where Z_R represents the impedance of a resistance; Z_C represents the impedance of the capacitor; Z_{CPE} represents the impedance of the constant phase element; Z_{total} represents the complete impedance of the equivalent circuit. The parameters of the equivalent circuit in Figure. 5 are summarized in Table 4. Among them, the calculation formula of R_p is $R_p = R_{ct} + R_c$ [27]. The value of R_p is determined by the corrosion resistance of the material. The larger the value of R_p, the better the corrosion resistance of the material. As listed in Table 3, the corrosion resistance of electroless NiP and NiP composite coatings were increased by more than one order of magnitude after coating. As shown in Fig. 6, the corrosion resistance of the coating has been increased after heat treatment.

$$Z_R = R \quad (1)$$

$$Z_C = \frac{1}{j\omega C} \quad (2)$$

$$Z_{CPE} = 1/Y_0(j\omega)^n \quad (3)$$

$$Z_{total} = R_s + \frac{j\omega C_{dl}R_{ct}R_c+R_{ct}+R_c}{Y_0(j\omega)^n(j\omega C_{dl}R_{ct}R_c+j\omega C_{dl}R_{ct}+R_{ct}+R_c+1)} \quad (4)$$

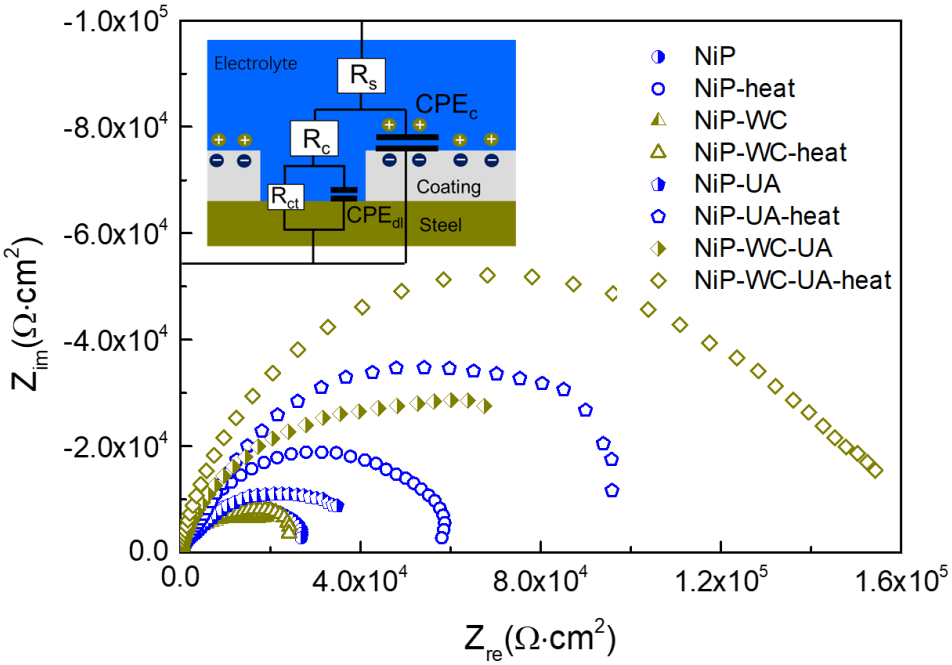

Figure 5. Nyquist plots and corresponding equivalent circuit of NiP coatings and NiP-WC coatings

Table 4. Parameters of the equivalent circuit in Figure 5

	R_s	CPE_c	n	R_c	CPE_{dl}	n	R_{ct}	R_p
NiP	121.9	1.70×10^{-5}	0.8747	1.54×10^{4}	7.99×10^{-5}	0.5469	1.65×10^{4}	3.19×10^{4}
NiP-heat	158	3.49×10^{-6}	0.868	2.59×10^{4}	1.42×10^{-5}	0.6399	3.70×10^{4}	6.29×10^{4}
NiP-WC	85.8	5.07×10^{-5}	0.8738	1.11×10^{4}	2.29×10^{-4}	0.636	1.64×10^{4}	2.75×10^{4}
NiP-WC-heat	103.2	1.88×10^{-5}	0.8651	1.09×10^{4}	9.90×10^{-5}	0.6228	2.06×10^{4}	3.15×10^{4}
NiP-UA	90.2	2.72×10^{-5}	0.3561	1.04×10^{2}	1.24×10^{-5}	0.774	6.11×10^{4}	6.12×10^{4}
NiP-UA-heat	87.97	1.35×10^{-5}	0.6356	3.68×10^{2}	6.15×10^{-5}	0.701	1.25×10^{5}	1.25×10^{5}
NiP-WC-UA	94.05	1.60×10^{-5}	0.3606	9.24×10^{1}	1.27×10^{-5}	0.896	1.49×10^{5}	1.49×10^{5}
NiP-WC-UA-heat	106.4	1.05×10^{-6}	0.8732	9.76×10^{4}	9.69×10^{-6}	0.4398	7.63×10^{4}	1.74×10^{5}

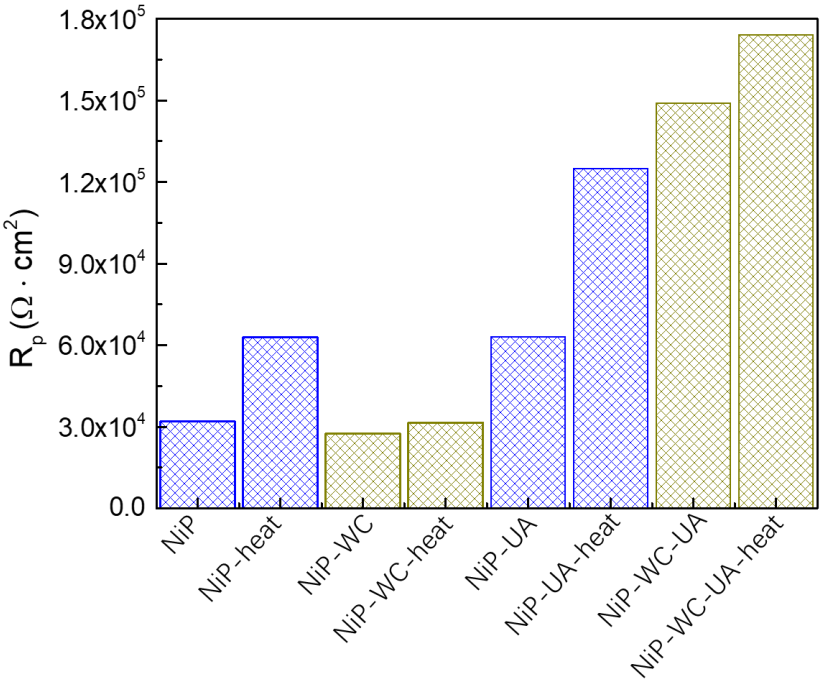

Figure 6. Polarization resistance (R_p) of NiP coatings and NiP-WC coatings

Figure. 7 shows the potentiodynamic polarization curve of the coatings by electroless plating, ultrasonically assisted electroless plating, and with and without heat treatment in a 3.5 wt. % NaCl solution. The corrosion potential (E_{corr}) and corrosion current density (I_{corr}) of electroless plating, ultrasonically assisted electroless plating, with and without heat treatment were determined by extrapolating the linear sections of the anodic and cathodic Tafel lines, and the electrochemical data are listed in Table 5. With ultrasonic assistance, E_{corr} moves in a positive direction and the I_{corr} values of the NiP and NiP-WC coatings decrease from 8.318×10^{-6}A/cm^2 to 2.939×10^{-6}A/cm^2 and 4.560×10^{-6}A/cm^2 to 3.228×10^{-6}A/cm^2. Respectively, this means that the corrosion resistance of the electroless coating was improved by ultrasonic assistance, which is ascribed to the dense structure of the coating prepared with ultrasonic assistance. However, the uneven distribution of P on the surface of the NiP coating during electroless plating leads to micro-galvanic cells, as shown in Fig. 8(a). As a result, the dynamic balance of Ni <—> Ni^{2+} + $2e^-$ was destroyed [28]. The I_{corr} of the coating was decreased after adding WC particles. This demonstrates that the corrosion rate of the electroless coating decreased after adding WC particles due to the WC particles forming a barrier by filling the very small pores present in the surface of the metal substrate in Fig. 8(b), thereby making the film denser and minimizing metal interactions in the solution. In addition, the NiP-WC coating with ultrasonic assistance in Fig. 8(c), forms uniformly distributed particles to increase the corrosion resistance of the coating. The heat treatment results demonstrate that E_{corr} values of the NiP and NiP-WC coating moved in a positive direction after heat treatment and the I_{corr} values of the NiP and NiP-WC coating decreased. Moreover, the I_{corr} values of the NiP-UA and NiP-WC-UA coating were decreased. This implies that the amorphous structure was loose before heat treatment. The crystalline structure densified after heat treatment, which increased the

corrosion resistance of the coating [29]. In addition, the Ni_3P phase in the electroless plating after heat treatment was evenly distributed in the coating, which can effectively prevent solution corrosion [30].

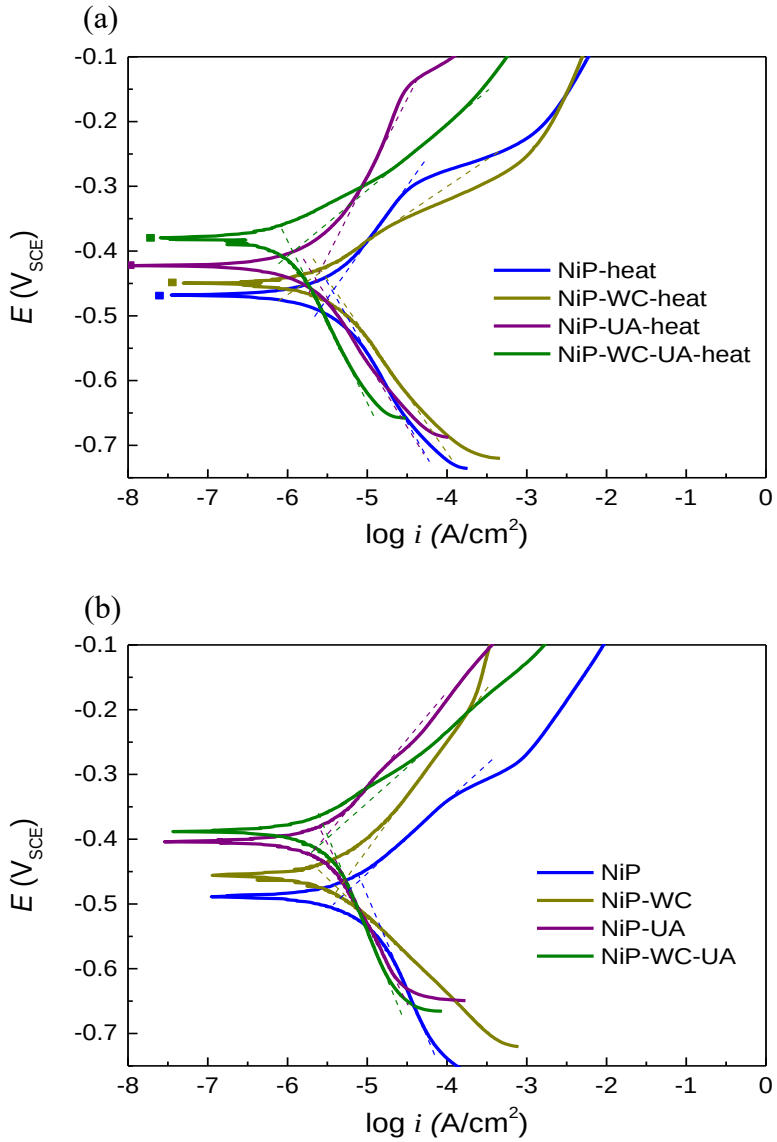

Figure 7. Potentiodynamic polarization curves of NiP coatings and NiP-WC coatings with heat treatment (a) and without heat treatment (b).

Table 5. Fitting parameters of the polarization curve in Fig. 7

samples	E_{corr} (V/SCE)	I_{corr} (A/cm^2)
NiP	-0.464	8.318×10^{-6}
NiP-heat	-0.462	3.707×10^{-6}
NiP-WC	-0.477	4.560×10^{-6}
NiP-WC-heat	-0.426	2.631×10^{-6}

NiP-UA	-0.397	2.939×10^{-6}
NiP-UA-heat	-0.442	2.280×10^{-6}
NiP-WC-UA	-0.398	3.228×10^{-6}
NiP-WC-UA-heat	-0.400	1.180×10^{-6}

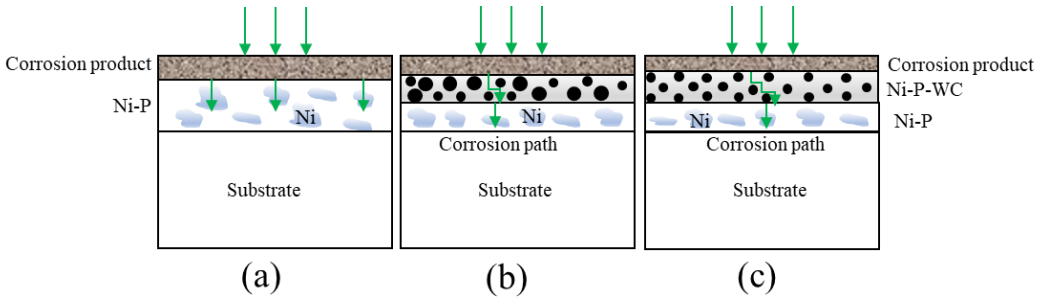

Figure 8. Schematic coating of the corrosion process (a) coating of NiP electroless plating with ultrasonic assistance (b) coating of NiP-WC electroless plating without ultrasonic assistance (c) coating of NiP-WC electroless plating with ultrasonic assistance

4. CONCLUSIONS

In this study, the preparation and properties of NiP-WC composite coating by ultrasonically assisted electroless plating were analyzed. The following conclusions were reached:

The microstructures of NiP and NiP-WC electroless coatings are denser and more uniform after ultrasonically assisted electroless plating. In addition, the thickness of the NiP electroless plating did not change after ultrasonically assisted electroless plating, while the thickness of the NiP-WC electroless plating increased. This is because ultrasonication can reduce the effect of WC particles on the growth rate via improved particle dispersion.

The hardness of the electroless plating coating was significantly improved by heat treatment, adding WC particles, and ultrasonic assistance. The main reason is that the crystal structure of the coating was transformed after heat treatment, and the microstructure of the coating was dense after ultrasonic assistance.

ACKNOWLEDGEMENT
This research was financially supported by National Natural Science Foundation (No. 51801167; No. 51774242); Project of Sichuan Department of Science and Technology (No. 20SYSX0179); Open Research Fund from State Key laboratory of Metal Material for Marine Equipment and Applicati on (SKLMEA-K201912); Young Elite Scientists Sponsorship Program by China Association for Science and Technology (YESS, No. 2018QNRC001), and Youth Scientific and Innovation Research Team for Advanced Surface Functional Materials, Southwest Petroleum University (No. 2018CXTD06).

References

1. Y.Z. Zhou, J.M. Zeng, J. Zhang, *Mater. Mech. Eng*., 35 (2008) 25.
2. L.H. Lu, D.J. Shen, J.W. Zhang, J. Song, L. Li, *Appl. Surf. Sci*., 257 (2011) 4144.
3. N. Zhou, Y. Ding, L.Q. Ma, *Electroplating & Pollution Control*, 33 (2013) 4.
4. P. Hang, Y.H. Shi, *Mater. Prot*., 43 (2010) 28.
5. F. Xue, L. Zhu, J.F. Wang, Z.B. Tu, G.L. Chen, *J. Zhejiang Sci-Tech Univ*., 33 (2015) 635.
6. C. Wei, T. Ren, *Surf. Technol*., 46 (2017) 91.
7. R.F. Zhuang, *Mater. Prot*., 30 (1997) 41.
8. A. J. Cobley, T. J. Mason, V. Saez, *T. Inst. Metal Finish*., 89 (2011) 303.
9. W.D. Zhang, Y. Wang, Z. Jiang, Y. Zhao, *Nat. Sci.,* 7 (2019) 60.
10. P. Zhou, W.B. Cai, Y.B. Yang, X.J. Li, T. Zhang, F.H. Wang, *Surf. Coat. Technol*., 374 (2019) 103.
11. J. Chen, G.L. Zhao, KenjiMatsuda, Y. Zou, *Appl. Surf. Sci*., 484 (2019) 835.
12. H.L. Wang, L.Y. Liu, Y. Dou, W.Z. Zhang, W.F. Jiang, *Appl. Surf. Sci.,* 286 (2013) 319.
13. Y.J. Li, R. Wang, F.M. Qi, C.M. Wang, *Appl. Surf. Sci*., 254 (2008) 4715.
14. J.G. Aha, D.J. Kim, J.R. Lee, H.S. Chung, C.O. Kim, H.T. Hai, *Surf. Coat. Technol*., 201 (2006) 3793.
15. Y.J. Chen, M.S. Cao, Q. Xu, J. Zhu, *Surf. Coat. Technol*., 172 (2003) 90.
16. G. Wen, Z.X. Guo, C.K.L. Davies, *Scr. Mater*., 43 (2000) 307.
17. R. Wang, W.C. Ye, C.L. Ma, C.M. Wang, *Mater. Character*., 59 (2008) 108.
18. J.P. Deepa, V.G. Resmi., T.P.D. Rajan, C. Pavithran, B.C. Pai, *Appl. Surf. Sci*., 257 (2011) 7466.
19. J.N. Balaraju, T.S.N. Sankara Narayanan, S.K. Seshadri, *Sol. State Electrochem*., 5 (2001) 334.
20. P.Y. Yang, L. Gong, B.S. Gu, H.J. Sun, *Surf. Technol*., 36 (2007) 61.
21. J.Z. Guo, J. Zhao, *Corros. Sci. Prot. Technol*., 29 (2017) 163.
22. H. Luo, M. Leitch, Y. Behnamian, Y.S. Ma, H.B. Zeng, J.L. Luo, *Surf. Coat. Technol*., 277 (2015) 99.
23. Q.H. Jia, G. Dan, *Ordn. Mater. Sci. Eng*., 42 (2019) 34.
24. W. Zhao, D.J. Kong, *Appl. Surf. Sci*., 481 (2019) 161.
25. G.K. Huang, L.D. Qu, Y.Z. Lu, Y.Z. Wang, H.G. Li, *Vacuum*, 153 (2018) 39.
26. L. Chen, S.L. Bai, Y.Y. Ge, Q.Y. Wang, *Appl. Surf. Sci.,* 456 (2018) 985.
27. Y. Zou, Z.W. Zhang, S.Y. Liu, D. Chen, G.X. Wang, Y.Y. Wang, M.M. Zhang, Y.H. Chen, *J. Electrochem. Soc.*, 162 (2015) 64.
28. Q.Y. Wang, S. Liu, Y.R. Tang, R. Pei, Y.C. Xi, D.X. Zhang, *Int. J. Electrochem. Sci*., 14 (2019) 3740.
29. H. Zhang, Q.C. Wang, Y.T. Dai, *Surf. Technol*., 33 (2004) 35.
30. Y.D. Wu, L.L. Zhang, *Foundry Technol*., 38 (2017) 577.